

⊕ Benefits of Makerspaces: Building An Enhanced Flight Mill for the Study of Tethered Insect Flight

Anastasia Bernat¹

Oct 16, 2020

¹Department of Ecology and Evolution, University of Chicago

1

Works for me

dx.doi.org/10.17504/protocols.io.bnclfmatn

Cenzer Lab at the University of Chicago

Anastasia Bernat

ABSTRACT

Makerspaces have a high potential of enabling researchers to develop new techniques and work with novel species in ecological research. This protocol demonstrates how to take advantage of the technology increasingly found in makerspaces in order to build a more versatile flight mill for a relatively low cost. Since this flight mill and trial design initially extracts its prototype from flight mills built in the last decade, this protocol instead focuses more on outlining divergences made from the simple, modern flight mill. As already shown, previous studies have made known how advantageous flight mills are to measuring flight parameters such as speed, distance, or periodicity and to allowing researchers to associate these parameters with morphological, physiological, or genetic factors. In addition to these advantages, I discuss the benefits of using the technology in makerspaces like 3D printers and laser cutters in order to build a more flexible, sturdy, and collapsible flight mill design. Most notably, the 3D printed components of this design allow the user to adjust the mill arm and IR sensor heights to test insects of various sizes and enable the user to easily disassemble the machine for quick storage or transportation to the field. Moreover, I emphasize making greater use of magnets and magnetic paint to attach insects with minimal stress during flight trials. Lastly, this protocol details a versatile analysis of flight data by programming how to efficiently take and process continuous but differentiable flight trials. Although more labor-intensive, community-shared makerspaces and free, online 3D modeling programs can help researchers avoid costly, pre-made products with narrowly adjustable dimensions. By taking advantage of the flexibility and reproducibility of technology in makerspaces, this protocol promotes creative flight mill design and inspires open science.

DOI

dx.doi.org/10.17504/protocols.io.bnclfmatn

PROTOCOL CITATION

Anastasia Bernat 2020. Benefits of Makerspaces: Building An Enhanced Flight Mill for the Study of Tethered Insect Flight. **protocols.io**
<https://dx.doi.org/10.17504/protocols.io.bnclfmatn>



KEYWORDS

flight mill, makerspace, 3D printing, laser cutting, automation, flight assay

LICENSE

This is an open access protocol distributed under the terms of the [Creative Commons Attribution License](https://creativecommons.org/licenses/by/4.0/), which permits unrestricted use, distribution, and reproduction in any medium, provided the original author and source are credited

CREATED

Oct 12, 2020

LAST MODIFIED

Oct 16, 2020

PROTOCOL INTEGER ID

MATERIALS TEXT

	Name of Material/ Equipment	Company	Catalog Number	Comments/Description
1	3D Printer	FlashForge	700355100638	It has Cloud, Wi-Fi, USB cable and Flash drive connectivity. Its slide-in build plate allows printed objects to be easily removed and all operations are commanded on a 3.5-inch color touchscreen. Free of charge at the makerspace.
2				
3	3D Printer Filament	FlashForge	PLA-1KG	Filament diameter 1.75 mm; 1kg/roll; any color. Free of charge at the makerspace.
4	Laser Cutter	Universal Laser Systems	PLS6.75	Free of charge at the makerspace.
5	Small Clear Vinyl Tubing	Home Depot	T10007005	Inner diameter 1/4 in; outer diameter 3/8 in; 20 ft long.
6	Large Clear Vinyl Tubing	Home Depot	T10007008	Inner diameter 3/8 in; outer diameter 1/2in; 20 ft long.
7	19 Gauge Non-Magnetic Hypodermic Steel Tubing	MicroGroup	304H19RW	19 Regular Wall (RW); alloy 304.
8	Filtered 20 uL Pipette Tip	Fisher Scientific	21-402-550	PP (Polypropylene); sterile.
9	Entomological Pins	BioQuip	120852	Size 2; diameter 0.45mm.
10	Acrylic Plastic Sheets	Blck Art Supplies	28945-1006	1.2 in x 24 in x 0.125 in. Laser cutter friendly.
	Hot Glue Gun with Hot Glue	Joann Fabrics	17366956	Cordless high temperature full size glue gun. Use with standard 7/16 diameter glue sticks in 4-inch or 10-inch lengths.
11			253-01-0860	50 sq ft.
12	Aluminum Foil	Target	B077HWSSXV	24 AWG Hook Up Wire 1007 PVC Solid wire; 24 gauge 300V Cable (32.8ft Each Color).
13	Electrical Wires	Striveday	84-031W	Stanley 6 in Bi-Material Long Nose Pliers.
14	Wire Cutters	Target	84-031W	Stanley 6 in Bi-Material Long Nose Pliers.
15	Solderless Breadboard	Adafruit	239	Full size MB-102 breadboard, 830 tie points. 2.2 in x 7 in (5.5 cm x 17 cm) with a standard double-strip in the middle and two power rails on both sides. Input voltage, DC 3.3 V 5 V.
16	180 Ω Resistor	E-Projects	10EP514180R	Carbon film, 1/4 Watt; 5% tolerance; flame retardant; stiff 24 gauge leads (0.022 in, 0.55 mm).
17	2.2 kΩ Resistor	Adafruit	2782	Carbon film, through-hole axial type, with 1/4 Watt max dissipation, 300V max voltage, 5% precision resistors, stiff 24 gauge lead.
18	IR Sensor	Adafruit	2167	This is the 3mm IR version. It works up to 25cm / 10". Can power it from 3.3V or 5V, but 5V will get better range. Dimensions: 20mm x 10mm x 8mm / 0.8 in x 0.4 in x 0.3 in.
19	Breadboard Power Supply	HandsOn Tech	MDU1025	A 3.3V and 5V Breadboard Power Supply Module with series diode, polarity reversal protection. The module can take 6.5V to 12V input and can produce 3.3V and +5V.
20	Power Adaptor	Adafruit	63	9 VDC 1000mA regulated switching power adapter. Fit for MB-102 Breadboard. Input voltage, DC 3.3V 5V.
21	DI-1100 USB Data Logger	DATAQ Instruments	DI-1100	Has 4 differential analog inputs with a +/- 10 V fixed measurement range. 20-40 kHz sample rate per channel. Includes WinDaq software.
22	Neoprene Rubber Sheet	Grainger	60DC16	One 1/8 in thick, 12 in x 12 in sheet is recommended.
23	Sophisticated Finishes Iron Metallic Surferacer Small Magnets	Blck Art Supplies	27105-2584	Contains 4 oz; covers 5 sq ft.
24		Bunting	N42P120060	Low-friction N42 neodymium, 0.120 in diameter, 0.060 in length, 0.5 lb holding force. Glued to the tethering end of the flight arm mill.
25	Large Magnets	Bunting	EP654	Low-friction N42 neodymium, 0.394 in diameter, 0.157 in length, 4.9 lb holding force. Used for magnetic bearing.
26	M5 Short Iron Screws	Home Depot	203540129	Philips Pan Head Stainless Steel Machine Screw; thread pitch .8 mm; screw length 10 mm; diameter 5 mm. Used to secure the 3D printed linear guide rail and block in place.
27	M5 Long Iron Screws	Home Depot	204283784	Philips Pan Head Stainless Steel Machine Screw; thread pitch .8; screw length 20 mm; diameter 5 mm. Used to secure the 3D printed linear guide rail and block in place.
28	M5 Hex Nut	Home Depot	204274112	Thread pitch .8; screw length; 20 mm 5 mm diameter.

Table 1. List of materials. Material name, company, catalog number, and description are listed for user purchasing.

ABSTRACT

Makerspaces have a high potential of enabling researchers to develop new techniques and work with novel species in ecological research. This protocol demonstrates how to take advantage of the technology increasingly found in makerspaces in order to build a more versatile flight mill for a relatively low cost. Since this flight mill and trial design initially extracts its prototype from flight mills built in the last decade, this protocol instead focuses more on outlining divergences made from the simple, modern flight mill. As already shown, previous studies have made known how advantageous flight mills are to measuring flight parameters such as speed, distance, or periodicity and to allowing researchers to associate these parameters with morphological, physiological, or genetic factors. In addition to these advantages, I discuss the benefits of using the technology in makerspaces like 3D printers and laser cutters in order to build a more flexible, sturdy, and collapsible flight mill design. Most notably, the 3D printed components of this design allow the user to adjust the mill arm and IR sensor heights to test insects of various sizes and enable the user to easily disassemble the machine for quick storage or transportation to the field. Moreover, I emphasize making greater use of magnets and magnetic paint to attach insects with minimal stress during flight trials. Lastly, this protocol details a versatile analysis of flight data by programming how to efficiently take and process continuous but differentiable flight trials. Although more labor-intensive, communally-shared makerspaces and free, online 3D modeling programs can help researchers avoid costly, pre-made products with narrowly adjustable dimensions. By taking advantage of the flexibility and reproducibility of technology in makerspaces, this protocol promotes creative flight mill design and inspires open science.

BEFORE STARTING

Given how intractable the dispersal of insects is in the field, the flight mill has become a common laboratory tool to address an important ecological phenomenon – how insects move. As a consequence, since the pioneers of the flight mill¹⁻⁴ ushered in six decades of flight mill design and construction, there have been noticeable design shifts that have occurred as technologies improved and became more integrated in scientific communities. Over time, automated data-collecting software replaced chart recorders and flight mill arms transitioned from glass rods to carbon rods and steel tubing⁵. In the last decade alone, magnetic bearings replaced Teflon or glass bearings as optimally frictionless and the pairing of versatile technology with the simple modern flight mill has been proliferating as audio, visual, and layer fabrication technology become increasingly integrated in researchers' workflows. These pairings have included high-speed video to measure

wing aerodynamics⁶, digital-to-analog boards to mimic sensory cues for studying auditory flight responses⁷, and 3D-printing to make a calibration rig for the study of wing deformation during flight⁸. With the recent rise of emerging technologies at makerspaces, particularly at institutions with digital media centers run by knowledgeable staff⁹, there are greater possibilities to enhance the flight mill to accommodate a larger range of insects, to test and analyze multiple insects, and to transport the device to the field. The flight mill presented here (adapted from Attisano and colleagues¹⁰) takes advantage of emerging technologies found in makerspaces not only to create flight mill components whose scales and dimensions are fine-tuned to the project at hand, but also to offer researchers a general and sufficient protocol in laser cutting and 3D printing without demanding a high-budget or specialized knowledge in computer aided design (CAD) models.

The benefits of coupling new technologies and methods with the flight mill is substantial, but flight mills are also valuable, stand-alone machines. Flight mills measure insect flight performance, allowing researchers to test how factors such as season, sex, age, host plant, population, body size, or morphological traits influence an insects' propensity to disperse. Distinct from alternative methods like actographs, treadmills, and the video recording of flight movement in wind tunnels and indoor arenas¹¹, the flight mill is notable for its ability to collect various flight performance statistics under laboratory conditions. As a viable proxy of insect flight performance, the flight mill has proven to be a key method in helping researchers progress in their disciplines whether that be directed towards integrated pest management¹²⁻¹⁴, population dynamics, genetics, biogeography, life-histories¹⁵, or phenotypic plasticity¹⁶⁻¹⁹. By comparing how flight speeds, distances, and periodicity differ by factors such sex, age, body size, or environmental conditions like temperature or humidity, there are various ways in which comparisons can be made to address important questions in insect flight behavior and dispersal. Other devices like high-speed cameras and actographs can require a strict, complicated, and expensive set-up, but can also lead to more fine-tuned movement parameters such as wing-beat frequencies and insect photophase activity²⁰⁻²¹. Thus, the flight mill presented here serves as a flexible, affordable, and customizable option for researchers to investigate flight behavior while integrating emerging technologies into their workflow.

In this paper, a design for an enhanced simple flight mill is described to aid researchers in their dispersal studies and to encourage the incorporation of emerging technologies in the field of behavioral ecology. This flight mill fits within the constraints of an incubator, holds up to eight insects simultaneously, automates data collection and processing, and minimizes stress placed on the insect when magnetically attached to the mill arm. Notably, its 3D printed enhancements allow the user to adjust the mill arm and IR sensor heights to test insects of various sizes and to disassemble the device for quick storage or transportation. Thanks to institutional access to a communal makerspace, all enhancements were free and, compared to the simple modern flight mill, no additional costs were accrued. All software needed are free, the electronic circuitry is simple, and all scripts, adapted from Attisano et al 2015¹⁰, can be modified to follow the specific needs of the experimental design. Lastly, coded diagnostics allow the user to check the integrity and precision of their recordings. With the assembly of the simple flight mill being already accessible, affordable, and flexible, the use of makerspace technologies to enhance the simple flight mill can grant researchers the space to overcome their own specific flight study needs and can inspire creative flight mill designs beyond this paper's considerations.

1 Build the Flight Mill in a Makerspace

Laser cut and assemble the acrylic plastic support structure.

- 1.1 Use eight 304.8 mm by 609.6 mm, 3.175 mm thick transparent acrylic sheets to construct the acrylic plastic support structure. Ensure that the material is not polycarbonate, which looks similar to acrylic but will melt instead of cut under the laser.
- 1.2 Locate the laser cutter in the makerspace. This protocol assumes the makerspace has a Universal Laser Systems (ULS) Platform Series (PLS) 6.75 Laser Cutter. For other laser cutters, read the laser cutter settings to determine what line color or thickness is needed to set the file lines to be laser cut or engraved (not to be rastered).

1.3 Open Adobe Illustrator, Inkscape (free), or another vector graphics editor. Prepare a file that reads the acrylic support design in a vector format with the aforementioned lines shown in **Figure 1**. File lines can be created in Adobe Illustrator in RGB mode with a line stroke of .0001 pt where RGB Red (255, 0, 0) cuts lines and RGB Blue (0, 0, 255) etches lines.

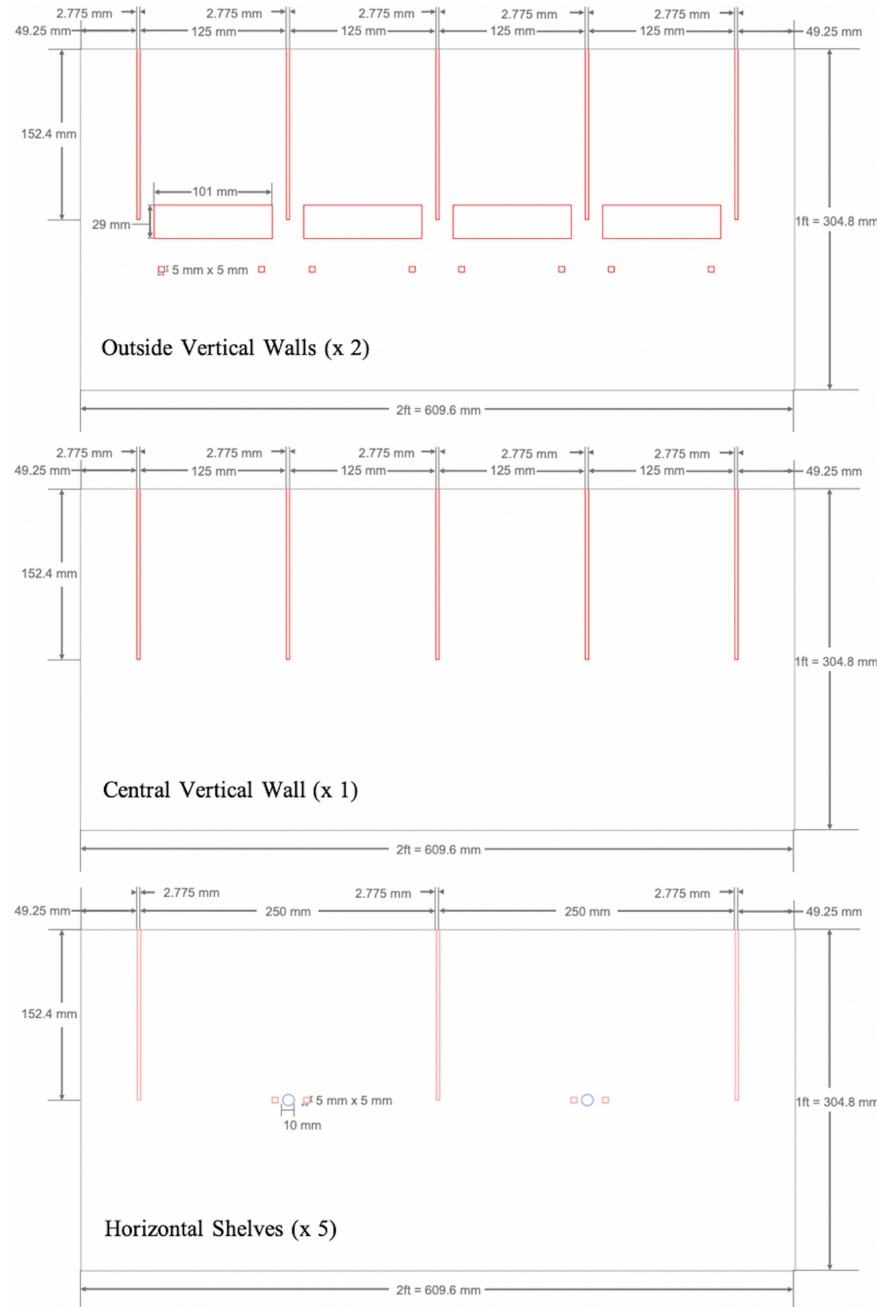


Figure 1. Designs to be laser cut for acrylic plastic sheet structure. Eight acrylic plastic sheets were laser cut in order to construct the plastic support structure of the flight mill. File lines were created in Adobe Illustrator in RGB mode where RGB Red (255, 0, 0) cut lines and RGB Blue (0, 0, 255) etched lines. For greater legibility in this figure, file line strokes were increased from .0001 pt to 1 pt. There are three different sheet designs: the outside vertical walls, a central vertical wall, and horizontal shelves. The two outside vertical walls slide into the horizontal shelves at their slits and their rectangular holes are used to mount the 3-D printed linear guide rail, blocks, and supports. There is one central vertical wall with slits that divides the flight mill into 8 cells and provides additional structural support. There are also five horizontal shelves with slits, an etched circle to mark the location of the magnetic tube supports, and small rectangular holes to allow the tube supports to be screwed in.

As a precaution, test and account for kerf for all slit and hole measurements, which can vary based on

- 1.4 the laser cutter's beam width, the width of the material, and the material type used. This can be done by designing and testing a kerf key (**Supplemental Files**).



Supplemental Figure 1. Kerf key. Kerf is the thickness of the material removed or lost in the process of cutting that material. For a laser cutter, two important factors will determine the width of the kerf: the beam width and the material type. To test and calculate the exact kerf, laser cut the key and fit the 20 mm width key into the slot that it fits most securely. Whichever width that is, subtract the width value from the key width value. For example, a key with width 20 mm that fits into a 19.5 mm slot will have kerf thickness of 0.5 mm.

- 1.5 Save the acrylic support designs and kerf key as file types that can be read by the laser software such as .AI, .DXF, or .SVG files. To send the job to the laser cutter, the user will need to print the file on the laser cutter's local machine and then open the laser software. If printed correctly, all the vector cutting lines in the design will appear with the appropriate corresponding colors in the laser software's control panel.
- 1.6 Select the material, in this case Plastic, and then the material type, Acrylic. For extra precision, measure the material thickness with a caliper and enter its thickness in the material thickness field. It is recommended to auto-enable the Z-Axis of the material's focal point, set the Figure Type to 'None', and leave the Intensity at 0%. Changing any advanced metrics on the laser cutter such as the laser % power or % speed will need to be further tested with the kerfkey.

Note: The rule of thumb is that the thicker the material, then the more power is required at a lower speed.

- 1.7 Before cutting, follow the makerspace's guidelines on powering up, using, and maintaining the laser cutter. Place materials in the printer cavity and cut the acrylic supports.

Note: To prevent possible eye damage, do not look at the laser or leave any acrylic sheet unattended while cutting.

- 1.8 Clean excess material out of the printer cavity and assemble the support structure. Assemble by inserting each horizontal shelf into the open slits of the outside vertical walls and central vertical wall as labeled in **Figure 2A**.

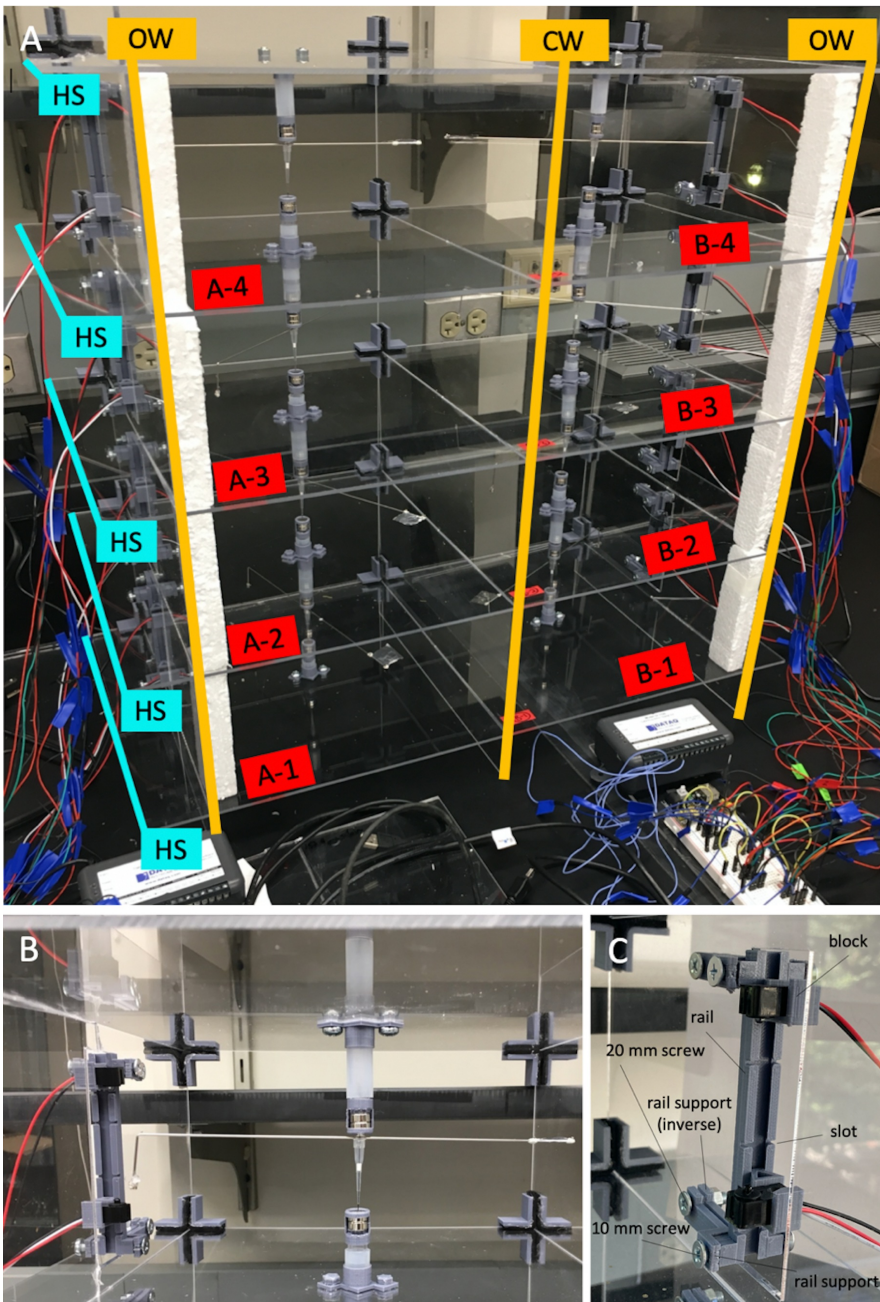


Figure 2. Assembled flight mill. **A.** Flight mill assembly. Each horizontal shelf (HS) has been inserted into the open slits of the outside vertical walls (OW) and central vertical wall (CW). Moreover, each cell, or 'chamber', is identified with a channel letter (A or B) that corresponds to a data logger and a channel number (1-4) that corresponds to the channel on the specific data logger. **B.** Flight mill cell assembly with flight mill arm. Magnetic bearings can be raised or lowered by sliding the inner tubes within the outer tubes to adjust the height of the arm. The IR sensors can be also be raised or lowered to align the sensors with the height of the flag on the arm. IR sensors can also be removed from their linear guide rail blocks easily if they need to be replaced or inspected or if the flight mill needs to be transported. Cross brackets provide structural support for each acrylic cell and can be easily inserted and removed. **C.** Linear guide rail and block assembly in the cell window with labeled components.

3D print the plastic supports.

1.9 Open a web browser and create a free account at Tinkercad.com, an online 3D modeling program.

1.10 Click on 3D Designs > Create a new design. To replicate this study's exact 3D printed designs as seen in **Figure 3**, download the archive 3D_Prints.zip (**Supplemental Files**) and move the folder onto the

desktop. Unzip and open the folder. In Tinkercad's workplane webpage, click on Import in the top right corner and select the .STL file(s).

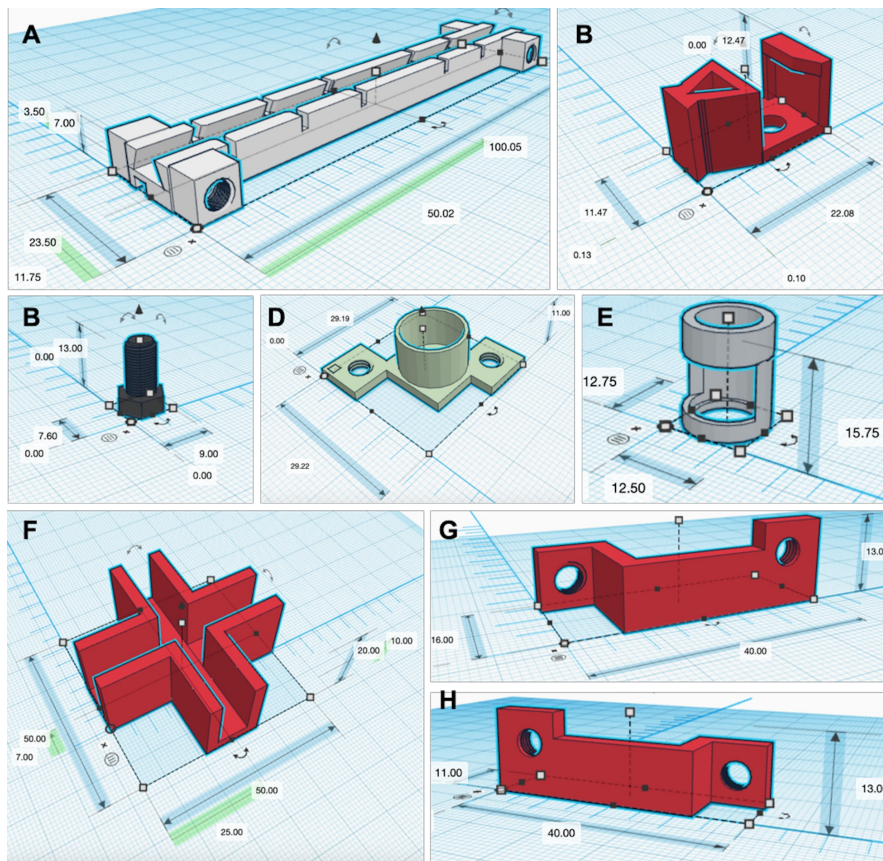


Figure 3. 3D printed designs. Measurements are in mm. **A.** Linear guide rail. **B.** Linear guide rail block shaped to hold an IR sensor. **C.** Screw used as support to replace iron screws. **D.** Tube support. **E.** Magnet support. **F.** Cross bracket used as an acrylic frame aligner and stabilizer. **G-H.** Supports to keep the linear guide rails in place (their mirrors not shown).

[3D_Prints.zip](#)

- 1.11 To self-create or make adjustments to the designs, follow the website's tutorials, make edits, and then export the new designs as .STL files. In total, 8 linear guide rails, 16 linear guide rail blocks, 12 to 20 screws, 15 cross brackets, 16 magnet holders, 16 tube supports, 16 short linear guide rail supports, and 16 long linear guide rail supports need to be 3D printed. To obtain the mirrors for all the linear guide rail related designs, click on the object, press M, and select the arrow corresponding to the object's width.

Note: See step 1.24 for more information on the linear guide rail pegs.

- 1.12 Download and install the free 3D printing slicing software, FlashPrint 4.4.0, to convert .STL files to a 3D printer readable .GX file. Other conversion software programs are acceptable, but this protocol assumes the makerspace is using a FlashForge Finder 3D Printer.
- 1.13 Double-click the icon of FlashPrint to start the software. Click Print > Machine Type and select the 3D Printer that is located in the makerspace.
- 1.14 Click the Load icon to load a .STL model file and the object will display on the build area.

- 1.15 Select the object and double-click the Move icon. Click “On Platform” to ensure that the model is on the platform. Click “Center” to place the object at the center of the build area or drag the object with the mouse pointer to position the object on the build area.
- 1.16 Click on the Print icon. Ensure that Material Type is set to PLA, supports and raft are enabled, Resolution is set to Standard, and that the temperature of the extruder matches the temperature suggested by the 3D Printer guide. The temperature can be changed within More Options >> Temperature.
- 1.17 Press OK and save the .GX file in the 3D_Prints folder or on a USB stick if the file cannot be transferred to the 3D Printer through USB cable.
- 1.18 Locate a makerspace’s 3D printing machine and ensure that the extruder is calibrated and there is enough filament for printing. Transfer the .GX file to the 3D Printer and print all types and quantities of plastic supports and enhancements. For each print, check that the filament is properly sticking to the plate.

Assemble 3D prints onto the acrylic support structure.

- 1.19 To visualize all the supports in place, see **Figure 2B**.
- 1.20 Hot glue 3.175 mm thick neoprene sheets onto the interior walls of the cross bracket. When dry, insert the cross brackets at the junctions of the acrylic shelves and the walls at the back of the device. This will help stabilize the flight mill.
- 1.21 Where possible, use 3D printed screws in order to minimize the magnetic influence of iron screws. Screw in the tube holders onto the bottom and top of each cell. Ensure that the top and bottom tube supports are aligned.
- 1.22 Insert a 30 mm long plastic tube (inner diameter (ID) 9.525 mm; outer diameter (OD) 12.7 mm) into the top tube support and a 15 mm long plastic tube (ID 9.525 mm; OD 12.7 mm) into the bottom tube support of each cell. Then, insert a 40 mm long plastic tube (ID 6.35 mm; OD 9.525 mm) into the top tube and a 20 mm long plastic tube (ID 6.35 mm; OD 9.525 mm) into the bottom tube. There should be strong enough friction between the tubes to hold the tubes in place, but not too much that the inner tube can still slide up and down if pulled on. If tubes are warped, submerge segments of the tubes for 1 minute in boiling water and insert them after they have been straightened out on a towel and have reached room temperature.
- 1.23 Place two low-friction N42 neodymium magnets (10 mm diameter; 4 mm length; 2.22 kg holding force) into a magnet support and insert the inner tube into the magnet support. Repeat on the bottom inner tube. Check to see that the magnets are repelling each other. Additionally, check that the inner tube is firmly lodged into each magnet support so that gravity acting on the magnets and magnet support is not strong enough to dislodge them from the inner tube.
- 1.24 Facing the same direction, slide two linear guide rail blocks into the linear guide rail. Lodge the linear guide rails and blocks upright into the windows on the outer vertical walls. Ensure that the block openings are facing upwards. To secure one linear guide rail in place, use two short linear guide rail supports, two long linear guide rail supports, four 10 mm long iron screws (M5; 0.8 thread pitch; 5 mm diameter), two 20 mm long iron screws (M5; 0.8 thread pitch; 5 mm diameter), and two hex nuts (M5; 0.8 thread pitch; 5 mm diameter). The full assembled linear guide rail is shown in **Figure 2C**.

Note: Open slots in the linear guide rail are intended to be used if and only if the linear guide rail becomes eroded by the repeated sliding of its block. If so, 3D print a small T-shaped peg found in the 3D_Prints folder.

Construct the pivoting arm. Sub-sections 1.25 and 1.26 are equivalent to sub-sections 1.2.2. and 1.2.3. in Attisano et al 2015 methods paper10. Instructions are described here again for ease of assembly.

- 1.25 Insert an entomological pin into a 20 μL filtered pipette tip to fix the pin in place. Slide the pin down enough such that both ends extend out the pipette tip to form the axis of the flight mill arm.
- 1.26 Cut a 24 cm length of 19 gauge non-magnetic hypodermic steel tubing. Hot glue the top of the pipette tip from step 1.25 to the center point of the tubing. Bend one end of the tubing at 2 cm from the end to an angle of 95°, leaving a long arm of 12 cm from the center point and a short arm with a 10 cm radius from the center to the bend.

Note: The radius length of the arm can be varied to accommodate different insect sizes.
Additionally, the bent ending of the arm can support different angles in order to position the insect in its natural flight orientation.
- 1.27 To test its magnetic suspension, position the arm at the top set of magnets. When properly positioned between the two magnets, the rotating arm should spin freely around the vertically suspended pin.
- 1.28 Glue two low-friction N42 neodymium magnets (3.05 mm diameter; 1.58 mm length; 0.23 kg holding force) on the bent end of the pivot arm, so that the metal-painted insect can be tethered for flight. On the unbent end of the pivot arm, wrap a piece of aluminum foil to create a flag. The foil flag will help act as a counterweight, and, due to its highly reflective properties, it will optimally break the IR beam sent from the IR sensor transmitter to the receiver.

Set up the IR sensor and data logger.

- 1.29 Place the IR sensor transmitter inside the top linear guide rail block with the source of the beam facing downwards. Then, place the IR sensor receiver inside the bottom block facing upwards.
- 1.30 On a solderless breadboard, connect the IR sensor transmitter and receiver in series with the data logger as shown in the electronic circuit in **Figure 4B**. Ensure that the IR sensor transmitter (not the receiver) input is connected first following the 180 Ω resistor. Place another 2.2k Ω resistor before the output of the IR receiver connection. Configure each channel's electronic circuit in alternate rows along the breadboard to minimize noise in voltage signal from multiple sensors during recording (**Figure 4A**).

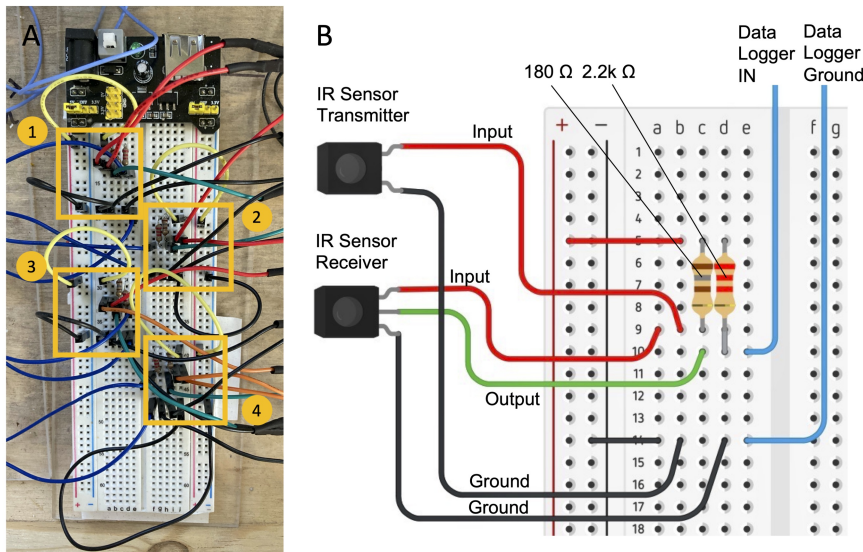


Figure 4. Flight mill electrical circuitry. A. Multiple electric circuits can be connected to a single breadboard in alternating rows. The size of the solderless breadboard limits how many flight cells can be accommodated. B. Simple diagram of electric circuit connecting the IR sensors to the data logger.

2 Conduct Flight Trials

Magnetically tether insects to the flight mill arm.

- 2.1 To minimize stress placed on the insect, apply magnetic paint on the insect's pronotum and let it dry for at least 10 minutes. Once dry, attach the insect to the flight mill arm magnets.

Note: For a stronger attraction between the insect and the arm magnets, apply multiple layers of magnetic paint.

- 2.2 Up to 8 insects can be flown at a time in the flight mill. Paint prep at least 16 insects in order to test multiple insects sequentially during a single recording session.
- 2.3 To remove the magnetic paint after testing, chip off the paint with fine forceps and dispose of it according to EPA and OSHA regulations.

Record multiple insects sequentially without terminating a recording session using WinDAQ's Event Marker Comment tool.

- 2.4 Download and install the free WinDAQ Data Recording and Playback Software.
- 2.5 Download the following Python scripts: split_files.py, standardize_troughs.py, and flight_analysis.py (**Supplemental Files**). Create a new folder titled Flight_scripts on the desktop and move the scripts into that folder.

[split_files.py](#)

[standardize_troughs.py](#)

[flight_analysis.py](#)

- 2.6 Create 5 new folders with the following exact names inside the Flight_scripts folder: data, files2split, recordings, split_files, and standardized_files. Download the datasheet.xlsx (**Supplemental Files**) and drag the file into the data folder in the Flight_scripts directory.



- 2.7 Use the datasheet.xlsx as a manual data-recording template. A minimum of four columns is needed: the identification number of the bug, whether the bug died before being tested, the recording set number, and the chamber comprised of the channel letter and channel number (e.g. "A-1", "B-4"). One possible chamber configuration is seen in **Figure 2A**.
- 2.8 Open the WinDAQ Dashboard, select the data-logger(s) from the checkbox list and press 'Start Windaq Software'. A new window will open for each data-logger selected and the input signal from each sensor will be shown.
- 2.9 To start a new recording session, press File > Record. Select the location of the recording file in the first pop-up window. Write the file name carefully. Files have to have at least the following in their names: the recording set number and channel letter. An example of a filename modeled in the Python scripts is the following: "T1_set006-2-24-2020-B.txt". Refer to split_files.py lines 78-87 from the Flight_scripts folder to get further details. Then, press OK.
- 2.10 In the next pop-up window, enter the anticipated length of the flight recording. Press OK when the insects are in a position to begin flight. Then, press Ctrl-S to finalize the file once the recording time has elapsed. Do not press Ctrl-S unless there is a need to terminate the recording early.

Note: If the file terminates too early either by typing Ctrl+S or the aforementioned length of time was too short, append a new recording to an existing file by clicking on File > Record. Select the file to append to and click "Yes" on the following pop-up window.

- 2.11 When pulling out tested insects during the recording, insert a commented event marker of the incoming insect at its selected chamber. Always manually record the ID, chamber, and recording set of the incoming insect in datasheet.xlsx before swapping insects.
- 2.12 To make an event marker comment, select the channel by clicking on the channel number. Then, click Edit > Insert Commented Mark. Define the comment with the identification number of the new insect entering the chamber. Press OK and load the insect into the chamber.

Visualize event marker comments and convert file from WDH to TXT.

- 2.13 Visualize event marker comments by going to Edit > Compression... and then clicking the "Maximum" button to fully compress the waveform into one window (**Figure 5A**).

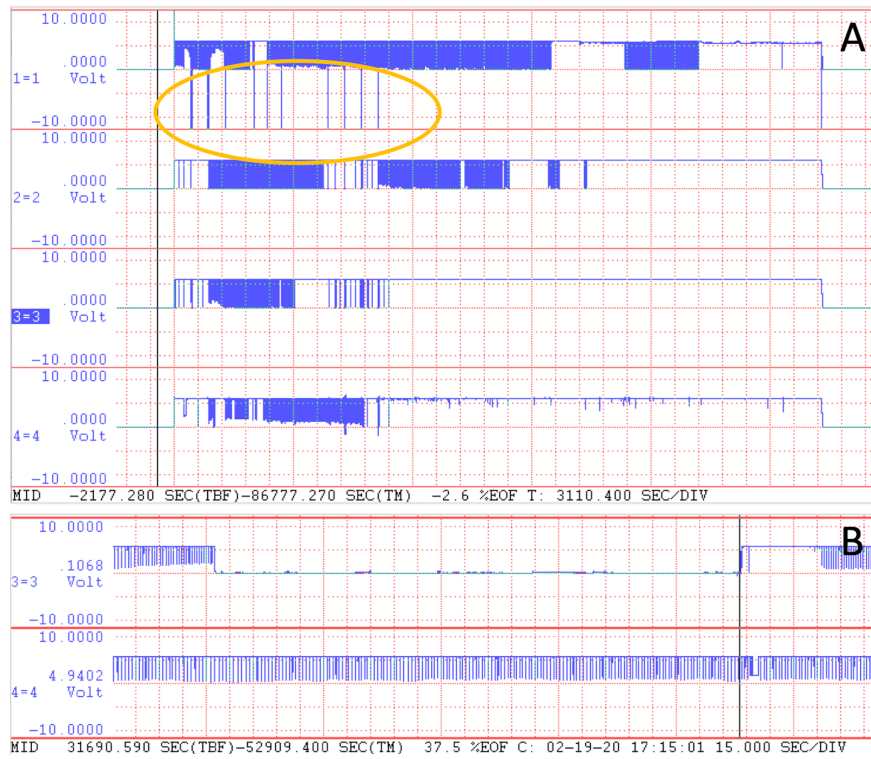


Figure 5. Examples of WDH flight recordings. Voltage troughs represent complete revolutions of the flight mill's arm. **A.** The seconds-per-division (sec/div) was changed from .2 sec/div to its max, allowing the entire waveform to be drawn across the screen. All event markers taken across all channels will only be visible in the first channel as lines that run from the max voltage to the bottom of the channel field window. All event makers for this recording set are within the yellow oval. **B.** In another recording set, the sec/div was changed from .2 sec/div to 15 sec/div to help visualize a recorded signal lost from 17:09 to 17:15 in channel 3. All other channels such as channel 4 continued to function properly.

- 2.14 Save the file in a .TXT format by going to File > Save As. Select the location to save the file, select the file type as "Spreadsheet print (CSV)" in the pop-up window, and write the filename with '.txt' at the end. In the following pop-up window, select "Sample Rate", "Relative Time", "Date and Time", and write "1" in between "Channel Number" and "Event Markers". Deselect all other options and click OK to save the file.

3 Analyze Flight Data

Split files by event marker comments.

- 3.1 Install the latest version of Python. All scripts in this protocol were developed on Python version 3.8.0.
- 3.2 Ensure that the following libraries are installed and up to date for the installed version of Python: csv, os, sys, re, datetime, time, and matplotlib.pyplot.
- 3.3 Drag all TXT file recordings into the recordings folder of the Flight_scripts directory.

- 3.4 Open the datasheet.xlsx file and save as a CSV by changing the file format to “CSV UTF-8 (Comma delimited)” if on Windows or “Macintosh Comma Separated” if on a Mac.
- 3.5 Open the split_files.py icon with the text editor of choice. If there is no preference, right-click on the script icon and select ‘Open with IDLE’.
- 3.6 Recode lines 133-135 and 232-233 if the user wrote a filename different from the suggested template (“T1_set006-2-24-2020-B.txt”). See lines 116-131 for an example on how to recode the script to accommodate different filenames, using the split() function.
- 3.7 In line 266, type the path to the Flight_scripts folder, and run the script. If the script successfully runs, the user will see, within the Flight_scripts directory, intermediate TXT files of mapped insect IDs generated in the files2split folder and TXT files for each insect tested in each recording set in the split_files folder. Additionally, in the Python Shell, users should see print statements of the filename, which insects are being swapped at a numbered event marker, and which files are being split and generated into new files by insect ID.

Standardize and select the troughs in the recorded signal as follows:

- 3.8 Open the standardize_troughs.py icon with the text editor of choice. If there is no preference, right-click on the script icon and select ‘Open with IDLE’.
- 3.9 In line 120, type the path to the Flight_scripts folder, and run the script. If the script successfully runs, the user will see files generated in the standardized_files folder in the Flight_scripts directory. All files should start with the “standardized_” and end with the original filename.
- 3.10 **Check the quality of the recordings:** Open the trough_diagnostic.png generated by the standardize_troughs.py located in the Flight_scripts folder. Ensure that all records are robust to changes in the minimum and maximum voltage value of the mean standardization interval. Recordings may have a lot of noise or have overly sensitive troughs if they exhibit large decreases in the number of troughs identified and counted when the minimum and maximum deviation values are increased.

Note: Additional diagnostics for the min-max normalization factor can also be coded, performed, and plotted. An alternative method for checking recording quality is described in steps 2.3.1. and 2.3.2. of the Attisano et al 2015 methods paper¹⁰.
- 3.11 After diagnostics have been assessed, uncomment out line 159 and specify the minimum and maximum deviation values, which define the minimum and maximum values around the mean voltage used to perform the standardization for all files. The default are deviation values 0.1 V.

Note: In line 45, the user can also specify the min-max normalization factor threshold in order to identify a voltage far below the threshold value.
- 3.12 Comment out lines 150 and 168 after inputting the deviation values and then run the script. The script will then run the standardizations efficiently for all files (approximately 40 times faster).

Analyze the flight track using the standardized file.

- 3.13 Open the flight_analysis.py icon with the text editor of choice. If there is no preference, right-click on the script icon and select ‘Open with IDLE’.

- 3.14 In lines 76-78, edit the optional speed correction that suppresses additional rotations of the mill's arm after an insect stops flying. Determine this threshold value with caution when working with slow flying insects.
- 3.15 In line 121, edit the speed thresholds to correct for false speed readings such as extremely fast speeds or negative speeds. In line 130, edit the time gap value to filter out long gaps that occur between two consecutive uninterrupted flying bouts.
- 3.16 In line 350, type the path to the folder in which the *.TXT standardized files are saved.
- 3.17 In line 353, input the arm radius length used during trials, which defines the circular flight path flown per revolution by the insect.
- 3.18 Identify the distance and time SI units as a string in lines 357 and 358.
- 3.19 In lines 388-397, use the split() function to extract, at minimum, the insect's identification number and the set number and chamber in which the insect flew from the filename. The script follows the comprehensive filename example of "standardized_T1_set006-2-24-2020-B.txt". However, this filename can be simplified as suggested in step 2.9 and variables like trial type on lines 392 and 401 can be commented out or deleted if not used.
- 3.20 Once all the user settings are specified, save the file and run the script. If the script successfully runs, the insect's corresponding ID number, chamber, and flight statistics calculated in the script will be printed in the Python Shell. Additionally, a flight_stats_summary.csv file similarly comprised of the information printed in the Python Shell is generated in the data folder of the Flight_scripts directory.

4 Representative Results

Flight data were obtained experimentally during Winter 2020 using field collected soapberry bugs *Jadera haematoloma* from Florida as the model insects (Bernat, A. V. and Cenzer, M. L. , 2020, unpublished data). Representative flight trials were conducted in the Department of Ecology and Evolution at the University of Chicago, shown below in **Figures 5-8**. The flight mill was set up within an incubator set to 28°C/27°C (day/night), 70% relative humidity, and a 14 hour light/10 hour dark cycle (sunrise at 8 AM and sunset at 10 PM). For each trial, the flight track of multiple bugs was recorded every hundredth of a second by the WinDAQ Software for up to 24 hours. Any individuals that did not exhibit continuous flight behavior at least within the last 10 minutes of its 30 minute testing phase were pulled off the flight mill and replaced with a new bug and its accompanying ID in an event marker comment. All bugs that exhibited continuous flight remained on the flight mill beyond 30 minutes until they stopped flying. Bugs were swapped until 4 PM each day. As represented in **Figure 8**, flight trials of single individuals in one day's worth of recording varied in length from 30 minutes to 20+ hours and were routinely asynchronous. By inserting event markers at the addition of new individuals, the process of this complex data structure becomes successfully automated in the split_files.py script.

The on-screen waveform and graphic diagnostic output also make it possible to identify gaps or resolve inconsistencies in the flight track data. **Figure 5A** shows the event marker comments made during recording and has successfully collected data for all channels without disruption. **Figure 5B** shows a moment where the recorded signal was lost in channel 3, dropping the voltage immediately to 0 V. This was possibly due to the crossing over of open wires or the loosening of wires. **Figure 6** compares three data files to show how noise or sensitive troughs in the recording data were diagnosed during the standardization process. The first (**Figure 6A**) is a file whose troughs generated by each

revolution of the flight mill arm were robust, meaning they largely deviated from the file's mean voltage. In turn, as the standardization interval around the mean increased, there was no change in the number of troughs identified. On the other side of the diagnostic spectrum, the third file (**Figure 6C**) had troughs that were either too sensitive or had extraneous voltage noise that did not deviate largely from the file's mean voltage. As a result, its number of troughs decreased substantially as the standardization interval around the mean increased. To check this individual's behavior, the original WDH recording file can be viewed to confirm whether it was truly flying.

By plotting the flight speed and duration statistics of the individual, flight behavior can be further characterized into four flight categories: bursts (B), bursts to continuous (BC), continuous to bursts (CB), and continuous (C) as represented in **Figure 7**. An individual that strictly exhibited continuous flight flew uninterrupted for 10 minutes or more at least by the end of its 30 minute testing phase (**Figure 7A**). An individual that flew sporadically throughout its 30 minute testing phase exhibited bursting flight (**Figure 7B**). An individual that initially strongly exhibited continuous flight for more than 10 minutes and then tapered within its 30 minute testing phase into sporadic bursts exhibited bursts to continuous flight (**Figure 7C**). Finally, an individual that initially demonstrated bursting flight and then transitioned into continuous flight for the remainder of the 30 minute testing phase and beyond exhibited bursting to continuous flight (**Figure 7D**). Thus, specific to the model insect and experimental framework, the user can use this graphic output to assess and identify general flight behavior patterns despite unique variations in individual tracks.

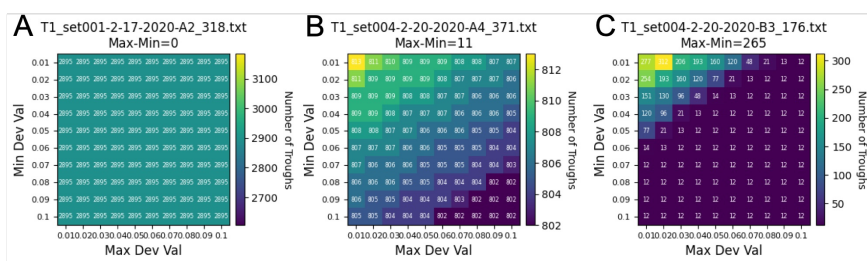


Figure 6. Representative trough diagnostic data from the soapberry bug *Jadera haematoloma*. Potential noise or overly sensitive troughs are readily recognized in the flight recordings. **A.** An optimal, robust recording from example individual 318. Since there was no change in the number of troughs as the minimum and maximum deviation values increased, the troughs were robust enough to be identified despite a large standardization interval. Thus, this file of insect ID 318 had no noise or sensitive troughs, and the user can be confident in the accuracy of the standardization. **B.** A sub-optimal, but still robust recording from example individual 371. There is a drop in the number of troughs as the minimum and maximum deviation values increased; however, the drop was minimal (12 troughs). There could be noise and some sensitive troughs but nothing substantial. **C.** A recording with noise or sensitive to changes in minimum and maximum threshold values from example individual 176. This diagnostic is different in that there is a clear and rapid drop in the number of troughs identified as the minimum and maximum deviation values increased until its number plateaus at 12 troughs. This signals potential noise or overly sensitive troughs while the 12 troughs remain as robust troughs. It would be advisable to look back into the original WDH recording file to confirm whether an insect, in this case ID 176, was truly flying.

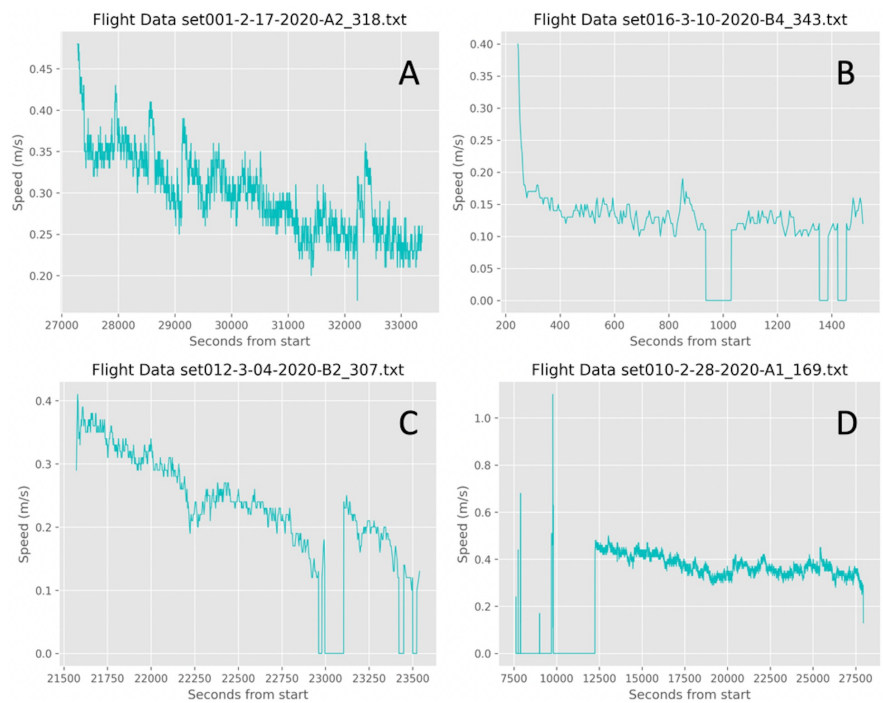


Figure 7. Representative flight data from the soapberry bug *Jadera haematoloma*. Four categories of flight behavior can be identified in the flight recordings. **A.** This individual flew continuously for 1.67 hours, beginning at high speeds and then tapering over time into lower speeds. **B.** This individual flew only in bursts within the first 30 minutes of their trial. Bursters can reach high speeds but this individual could only retain low speeds. **C.** This individual had maintained continuous flight for 25 minutes and then tapered off into bursts for the remaining 5 minutes of their trial. **D.** This individual began as a burster, reaching high sporadic speeds, and then transitioned into continuous flight for about 4 hours.

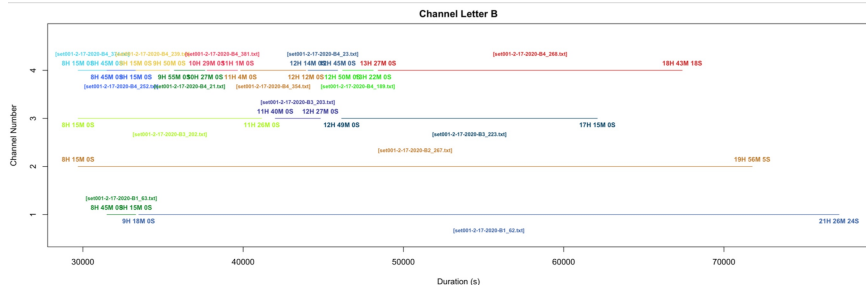


Figure 8. Representative channel visualization of multiple flight trials within a single recording set. Each color represents an individual soapberry bug, *Jadera haematoloma*, at its given channel letter and channel number during its trial. All start times, stop times, and filenames were extracted from each individual's unique flight track TXT file.

5 Discussion

The simple, modern flight mill provides a range of advantages for researchers interested in studying the flight behavior of a model species by delivering a reliable and automated design that tests multiple insects efficiently and cost-effectively^{10,22}. Likewise, there is a strong incentive for researchers to adapt to fast-emerging technologies and techniques from industry and other scientific fields to design and build experimental tools to study ecological systems^{9,23-24}. This protocol takes advantage of two rapidly emerging technologies, the 3D printer and the laser cutter, which are becoming increasingly available in communal makerspaces, in order to enhance the simple, modern flight mill. These enhancements provide a more flexible, adjustable, and collapsible design that accommodates insects of different sizes, minimizes stress placed on the insect, and allows the flight mill to be transported easily to multiple locations or environments. Furthermore, the additional expenses of using the technologies are minimal or even free. However, these technologies can also be a challenge to experiment with if their accessibility or reaching proficiency in using vector graphics editors and 3D image software is not readily available. In turn, the flight mill presented here serves to both encourage researchers to incorporate available emerging technologies in their workflow and allow researchers to build a customizable, flexible, and effective flight mill without specialized knowledge of electronics,

programming, or computer aided design (CAD) models.

The strongest aspects of this protocol are the makerspace's technologies that expand a user's flight mill design options, the use of magnetic paint to minimize insect stress, and the automation of flight recordings followed by the processing of multiple insects within a single recording. The laser cutter offers precise and exact cutting capabilities that can handle jobs of almost any complexity. The user can modify the acrylic support structure to mount additional 3D prints or purchased items. The 3D printer allows the user to create customizable flight mill components that can bypass costly, pre-made products with narrowly adjustable dimensions. Finally, the use of automated recording software and Python scripts to differentiate multiple flight trials within a single recording makes it possible to study sporadic bouts of flight to very long bouts of flight. However, given how variable flight activity and duration is across species, it is suggested that the user conducts preliminary trials in order to understand the limits and general patterns of a species' flight behavior so as to optimize data collection. The user can also assess the integrity of their recordings using the diagnostic graphic output and can account for any necessary speed corrections in the scripts.

Researchers should also be aware of the flight mill's general constraints. Previous studies have made known and have attempted to remediate the limitations of tethered flight including a lack of tarsal contact to allow the insect to rest at will^{15,22}, the absence of energy expended when an insect takes-off²⁵, the additional drag the insect overcomes when pushing the flight mill arm, and the insect needing to compensate for the outward aerodynamic forces experienced due to the centrifugal acceleration of its circular flight track^{6,26}. Additionally, there continues to be inconsistencies on how to categorize or more precisely quantify the short or 'trivial' bursts insects display, especially when considering the flight behavior and mechanisms of large migratory insects to those of small insects who exhibit mostly hovering flight^{21,27-28}. Despite these limitations, there has been significant progress in capturing and categorizing flight behavior within insect species and researchers have continued to couple the flight mill with other technologies and methods⁶⁻⁸.

Flight mills have played an important role in enabling researchers to understand the dispersal of insects – an ecological phenomenon still essentially intractable in the field. Future advances in the design and application of the flight mill can be achieved as researchers become more proficient in emerging technologies and the software accompanying those technologies. This could include designing flight mill arm bearings that allow vertical lift or gives the insect greater flight orientation flexibility. Additionally, the precision of laser cutters and 3D printers may be necessary for researchers interested in scaling down and calibrating for small insects with mostly hovering capabilities. In turn, the goal of this protocol was to provide an easy entry to these technologies while constructing one of the most common and useful devices in the field of behavioral ecology – the flight mill. If researchers have access to a communal makerspace and are committed to navigating its technologies, the resulting enhancements and improvements of the modern flight mill will lead to creative and collaborative flight mill design and will continue to offer insights into the underlying traits and mechanisms that influence insect species' variations and patterns in movement.

6 Acknowledgements

I would like to thank Meredith Cenzer for purchasing all flight mill materials and providing continuous feedback from the construction to the write-up of the project. I would also like to thank Ana Silberg for her contributions to standardize_troughs.py. Finally, I would like to thank the Media Arts, Data, and Design Center (MADD) at the University of Chicago for permission to use its communal makerspace equipment, technology, and supplies free of charge.

7 References

1. Krogh, A., Weis-Fogh T. Roundabout for studying sustained flight of locusts. *Journal of Experimental Biology.* **29**, 211-219 (1952).
2. Hocking, B. The intrinsic range and speed of flight of insects. *Transactions of the Royal Entomological Society of London.* **104**, 223-345 (1953).
3. Chambers, D. L., O'Connell, T. B. A flight mill for studies with the mexican fruit fly. *Annals of the Entomological Society of America.* **62**(4),917-920 (1969).
4. Chambers, D. L., Sharp, J. L., Ashley, T. R. Tethered insect flight: A system for automated data processing of behavioral events. *Behavior Research Methods & Instrumentation.* **8**(4), 352-356 (1976).
5. Naranjo, S. E. Assessing insect flight behavior in the laboratory: a primer on flight mill methodology and what can be learned. *Annals of the Entomological Society of America.* **112**, 18-199 (2019).
6. Ribak G., Barkan S., Soroker V. The aerodynamics of flight in an insect flight-mill. *PLoS ONE.* **12**(11), e0186441 (2017).

7. Pollack G.S., Martins, R. Flight and hearing: ultrasound sensitivity differs between flight-capable and flight-incapable morphs of a wing-dimorphic cricket species. *The Journal of Experimental Biology.* **210**, 3160-3164 (2007).
8. Koehler, C., Liang, Z., Gaston, Z., Wan, H., Dong, H. 3D reconstruction and analysis of wing deformation in free-flying dragonflies. *The Journal of Experimental Biology.* **215**, 3018-3027 (2012).
9. Behm, J. E., Waite, B. R., Hsieh, S. T., Helmus, M. R. Benefits and limitations of three-dimensional printing technology for ecological research. *BMC Ecology.* **18**, 1-13 (2018).
10. Attisano, A., Murphy, J. T., Vickers, A., Moore, P. J. A simple flight mill for the study of tethered flight in insects. *Journal of Visualized Experiments.* **106**, doi:10.3791/53377 (2015).
11. Reynolds, D. R., Riley, J. R. Remote-sensing, telemetric and computer-based technologies for investigating insect movement: a survey of existing and potential techniques. *Computers and Electronics in Agriculture.* **35**, 271-307 (2002).
12. Davis, M. A. Geographic patterns in the flight ability of a monophagous beetle. *Oecologia.* **49**, 1-6 (1986).
13. Taylor, R. A. J., Bauer, L. S., Poland, T. M., Windell, K. N. Flight performance of *Agrilus planipennis* (Cleoptera: Buprestidae) on a flight mill and in free flight. *Journal of Insect Behavior.* **23**, 128-148 (2010).
14. Irvin, N. A., Hoddle, M. S. Assessing the flight capabilities of fed and starved *Allograpta obliqua* (Diptera: Syrphidae), a natural enemy of Asian citrus psyllid, with computerized flight mills. *Florida Entomologist.* **103**(1), 139-140 (2020).
15. Minter, M. et al. The tethered flight technique as a tool for studying life-history strategies associated with migration in insects. *Ecological Entomology.* **43**, 397-411 (2018).
16. Dingle, H., Blakley, N. R., Miller, E. R. Variation in body size and flight performance in milkweed bugs (Oncopeltus). *Evolution.* **34**(2), 371-385 (1980).
17. Martini X., Hoyte, A., Stelinski, L. L. Abdominal color of the Asian citrus psyllid (Hemiptera: Liviidae) is associated with flight capabilities. *Annals of the Entomological Society of America.* **107**(4), 842-847 (2014).
18. Chen, M. et al. Flight capacity of *Bactrocera dorsalis* (Diptera: Tephritidae) adult females based on flight mill studies and flight muscle ultrastructure. *Journal of Insect Science.* **15**(1), doi: 10.1093/jisesa/iev124 (2015).
19. Guo, J., Li, X., Shen, X., Wang, M., Wu, K. Flight performance of *Mamestra brassicae* (Lepidoptera: Noctuidae) under different biotic and abiotic conditions. *Journal of Insect Science.* **20**(1), 1-9 (2020).
20. Johnson, M. W., Toscano, N. C., Jones, V. P., Bailey, J. B. Modified ultrasonic actograph for monitoring activity of lepidopterous larvae. *Proceedings of the Hawaiian Entomological Society.* **27**, 141-146 (1986).
21. Cheng, X., Sun, M.A. Wing-kinematics measurement and aerodynamics in a small insect in hovering flight. *Scientific Reports.* **6**(25706), doi: 10.1038/srep25706 (2016).
22. Jones, H. B. C., Lim K. S., Bell, J. R., Hill, J. K., Chapman, J. W. Quantifying interspecific variation in dispersal ability of noctuid moths using an advanced tethered flight technique. *Ecology and Evolution.* **6**(1), 181-190 (2016).
23. Walker, M., Humphries, S. 3D Printing: applications in evolution and ecology. *Ecology and Evolution.* **9**, 4289-4301 (2019).
24. Shahrbudin, N., Lee, T. C., Ramlan, R. An overview of 3D printing technology: technological, materials, and applications. *Science Direct.* **35**, 1286-1296 (2019).
25. Taylor, R. A. J., Nault, L. R., Styler, W. E., Cheng, Z. B. Computer-monitored, 16-channel flight mill for recording the flight of leafhoppers (Homoptera: Auchenorrhyncha). **85**(5), 627-632 (1992).
26. Nachtigall, W., Hanauer-Thieser, U., Mörz, M. Flight of the honey bee VII: metabolic power versus flight speed relation. *Journal of Comparative Physiology B.* **165**, 484-489 (1995).
27. Hardie, J. Flight behavior in migrating insects. *Journal of Agricultural Entomology.* **10**(4), 239-245 (1993).
28. Blackmer, J. L., Naranjo, S. E., Williams, L. H. Tethered and untethered flight by *Lyrgus Hesperus* and *Lyrgus lineolaris* (Heteroptera: Miridae). *Environmental Entomology.* **33**(5), 1389-1400 (2004).